

AXIAL CAPACITY OF BARRETTE PILES EMBEDDED IN GRAVEL LAYER

San-Shyan Lin¹, Fang-Chih Lu², Chin-Jung Kuo³, Tzi-Wei Su⁴, and Erica Mulowayi⁵

ABSTRACT

In this paper, the axial performance of two heavily instrumented barrette piles, with and without grouting, socket into gravel layer in Taipei are evaluated based on the results of pile load tests. Both piles are 44 m long with the same dimension of 0.8 by 2.7 m, installed by hydraulic long bucket. One of the piles with toe grouting was socket 6 m into gravel layer and the other pile without toe grouting was socket 3 m into gravel layer. The load versus displacement relationships at pile head, the $t-z$ curves of upper soil layers and of bottom gravel layer, and the tip resistance versus displacement relationships are important concerns and are presented in the paper. The $t-z$ curves interpreted from the measured data along depth are also simulated by the hyperbolic model.

Key words: Barrette piles, pile load test, toe grouting.

1. INTRODUCTION

Although cylindrical drilled shaft is the most common type of pile foundation adopted by local engineers to support high rise buildings in Taipei, Taiwan. In the past few years, increasing numbers of barrette pile have also been used. It's believed, under the same excavated soil volume in the hole, the barrette pile provides higher bearing capacity than that of the cylindrical drilled shaft. In addition, the rectangular pile can also be used to control the deformation of slurry wall (Liao *et al.* 2013).

In some area of Taipei City, over tens of meters thick of gravelly soil layer sandwiched between top soil layer and bottom bedrock are often found. Use of rock or gravel layer socket drilled shafts in building projects has been increased in Taipei in the past decade. How to estimate side friction resistance of shaft through gravelly soil layer have been major concerns of local geotechnical engineers. Especially the ground investigation of the gravel layer, located tens of meter below soil layer, was conducted by SPT test only and resulted in invalid high SPT-N value. Bearing capacity of drilled shafts in gravel formation has also drawn geotechnical engineer's attention worldwide, such as the available researches by Stas and Kulhawy (1984) and O'Neill and Reese (1999). Rollins *et al.* (2005) conducted a series of uplift tests on drilled shaft in soil profiles ranging from uniform sand to sandy gravel to evaluate side friction in gravel soils. These researches were all focused on the gravel layer right under the ground surface.

To compare the axial performance of two barrette piles embedded in gravel layers, two compressive tests were conducted at

Manuscript received August 2, 2014; revised November 14, 2014; accepted November 20, 2014.

¹ Professor (corresponding author), Department of Harbor and River Eng., National Taiwan Ocean University, Keelung, Taiwan 20224 (e-mail: ssln46@gmail.com).

² Manager, Ground Master Construction Co. Ltd, Taipei, Taiwan.

³ Manager, Mice Engineering Consultants Co. Ltd, Taipei, Taiwan.

⁴ Graduate student, Department of Harbor and River Eng., National Taiwan Ocean University, Keelung, Taiwan 20224.

⁵ Graduate student, Queensland University of Technology, Australia.

two different sites in Taipei. Both piles, 0.8 m by 2.5 m, were 44 m long and were heavily instrumented with strain gages. One of the piles, C1 pile with toe grouting at site 1, was socket 6m into gravel layer. The other pile without toe grouting, C2, was socket 3 m meter into gravel layer at site 2. Performance of the two tested piles was evaluated based on the loading test results. Effect of toe grouting was also evaluated by comparing the performance between C1 and C2 piles. The $t-z$ curves of the frictional resistance of both piles were also studied and characterized using the hyperbolic model.

2. SUBSURFACE CONDITIONS

The standard penetration test and ground investigation were carried out at both test sites. At site 1, in addition to top 1m of backfill material, from ground surface down consists of 39 m of alternate low plasticity clay layer and silty sand layer. Beneath the soil layers, gravel formation is encountered.

The subsurface condition of site 2 is similar to the site 1. In addition to top 5 m of backfill material, typical soil conditions at the site from ground surface down consists of 39 m of alternate low plasticity clay layer and silty sand layer. Again, beneath the soil layers, gravel formation is encountered. Typical subsurface soil physical and strength properties of both sites are presented in Table 1. The SPT-N value at gravel of site 1 was 17 to higher than 50. At site 2, the SPT-N values were all higher than 50.

3. BARRETTE PILE CONSTRUCTION AND TESTING SETUP

The Masago hydraulic long bucket was used for installation of both piles. Drilling was done with polymer slurry pumped into a pile borehole while the slurry-soil mixture was discharged from the air-lift riser pipe to allow settlement in the tank to facilitate the removal of soil particles. Both piles were concreted using tremie method. Six 5.08cm PVC pipes were attached to the rebar cage of each pile for sonic logging integrity testing.

Table 1 Physical properties and strength of the soil strata

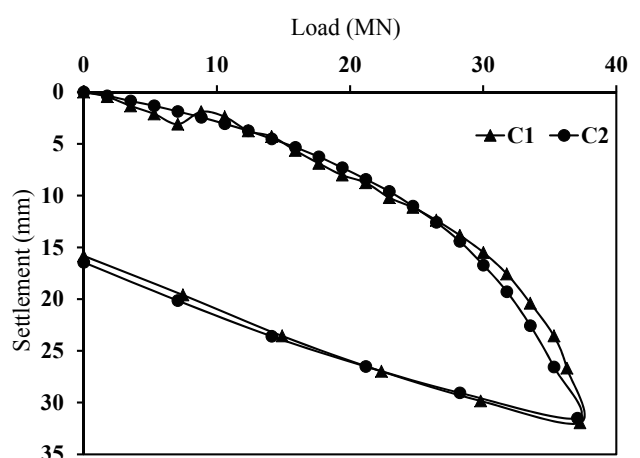
Shaft	Layer	Depth (m)	Classification	SPT N	γ_i (kN/m ³) (unit weight)	c' (kN/m ²)	ϕ' (°)	S_u (kN/m ²)
C1	1	0 ~ 1	SF	—	18.64	0	28	
	2	1 ~ 4.9	CL	2 ~ 7	18.64	0.98	26	24.53 ~ 29.43
	3	4.9 ~ 13.4	SM	5 ~ 21	18.74	0	30	
	4	13.4 ~ 20.7	CL	3 ~ 9	18.44	0.98	27	39.24 ~ 58.86
	5	20.7 ~ 22.7	ML/SM	8 ~ 14	18.74	0	31	
	6	22.7 ~ 30.5	CL	6 ~ 15	19.13	0.98	30	78.48 ~ 117.72
	7	30.5 ~ 34.4	ML/SM	10 ~ 37	19.13	0	32	
	8	34.4 ~ 38.4	CL	8 ~ 27	19.03	9.8	30	117.72 ~ 176.58
	9	> 38.4	GW	17 ~ > 50	—	—	—	
C2	1	0 ~ 5.1	SF/CL	2 ~ 4	18.44	0	28	12.75
	2	5.1 ~ 15.1	SM	3 ~ 22	19.42	0	30	
	3	15.1 ~ 20	CL/ML	6 ~ 13	18.74	0	30	
	4	20 ~ 27.1	SM	11 ~ 27	19.03	0	31	
	5	27.1 ~ 38.5	CL/ML	8 ~ 19	18.93	0	30	
	6	38.5 ~ 41	SM	20 ~ 27	19.23	0	32	
	7	> 41	GM	> 50	—	—	—	

To evaluate the total load carried at different depths along the pile, rebar gages were installed at pre-selected depths of each pile. The selected levels of C1 pile were 1.5, 17.25, 23, 30.4, 32.5, 35, 38.4, 39.65, 40.9, 42.15, and 43.4 m deep below ground level. For the C2 pile, the selected levels were 2, 26.45, 28.4, 30.44, 33.6, 36.8, 40.8, 42.5, 43.2 m below ground level. The gages were attached to the rebar cage in sets of eight and six at each depth of site 1 and site 2 shafts, respectively. Given modulus of pile section, load distribution along pile can be assessed assuming same axial strain is developed in concrete and steel. Since the cut-off level is 17.25 m and 26.45 m of C1 and C2 piles, respectively, both piles were also installed with rod extensometer at level of 17.25 m and 26.45 m plus additional level of 43.4 m and 43.2 m.

Pile toe grouting was conducted for C1 pile via pre-installed two steel pipes. A high pressure water jet, 17658 to 21582 kPa, was used first to clean undesirable material from the pile base. After cleaning of the base sediment had been completed, the grout injected through one of the base grouting holes. The water cement ratio was 1 by 1. In addition, the grouting pressure was also maintained between 17658 to 21582 kPa. The quick test procedure of ASTM D1143 was followed for compressive tests. Pile load tests were carried out 67-day and 68-day after the installation of the piles C1 and C2, respectively. Arrangement of the test setup of the C2 shaft is shown in Fig. 1. The test setup of the C1 shaft is similar to the C2 shaft for the same size.

4. TEST RESULTS AND DISCUSSION

The load versus settlement relations at pile head of both piles are presented in Fig. 2. As shown in the figure, the load-settlement relationships of both piles are almost identical through the full loading stage. When the maximum applied loading of C1 was reached 38 MN, the corresponding displacement increased up to 32 mm at the head and 17.48 mm at the toe. For C2 shaft, the displacement reached 31.51 mm at the head and 17.96 mm at the toe under the applied loading of 37.80 MN. Although the pile C1 embedded deeper into gravel layer and improved by toe

**Fig. 1 Arrangement of the test setup of the C2 shaft****Fig. 2 Pile head movement of the test piles C1 and C2**

grouting, the capacity of the C1 is the same as the C2 pile. It's possibly due to the gravel layer at site C2 has higher SPT-N values than that of site C1, which includes SPT-N value as low as 17 only. Unit end bearing resistance versus toe displacement relations of both C1 and C2 shafts are shown in Fig. 3. Higher end bearing resistance of C1 is also observed due to toe grouting improvement. As shown in Fig. 3, the results of C1 is almost parallel to that of the C2, under the same displacement, the end bearing resistance of C1 is roughly 1.5 times higher than that of C2.

The axial load transfer along depth of C1 and C2 is given in Fig. 4 for comparison. Each pile appeared to have different load distribution rate. Under the same applied load at head, in general higher frictional resistance was mobilized by C1 pile.

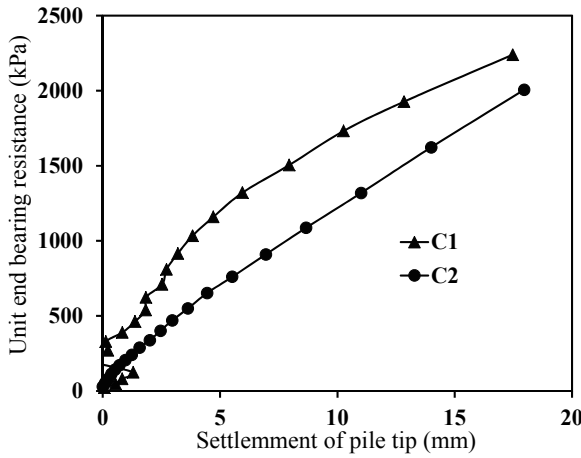


Fig. 3 Mobilized unit bearing versus settlement relationship of the piles C1 and C2

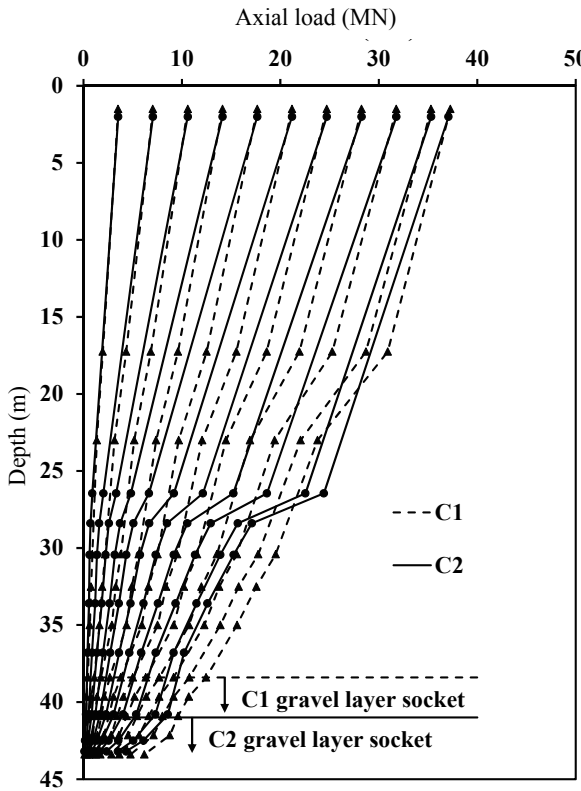


Fig. 4 Load distribution of tested piles C1 and C2

Based on the De Beer and the Van der veen method, the ultimate capacity of the C1 pile is 35.28 MN and 41.16 MN, respectively. For C2 pile, the ultimate capacity is higher than 37.04 MN and 39.20 MN with respect to the De Beer and the Van der veen method.

The t - z curves of the soil layer and the gravel layer at various elevation of C1 and C2 piles are given in Figs. 5 and 6, respectively. The shaft frictional resistance of the clay layer is in the range between 50 and 125 kPa. In addition, the shaft frictional resistance of the gravel layer is up to 250 kPa and 350 kPa of C1 and C2 shaft, respectively. Higher shaft frictional resistance of the gravel layer at C2 shaft is another evidence that the C2 shaft has better performance than that of the C1 shaft.

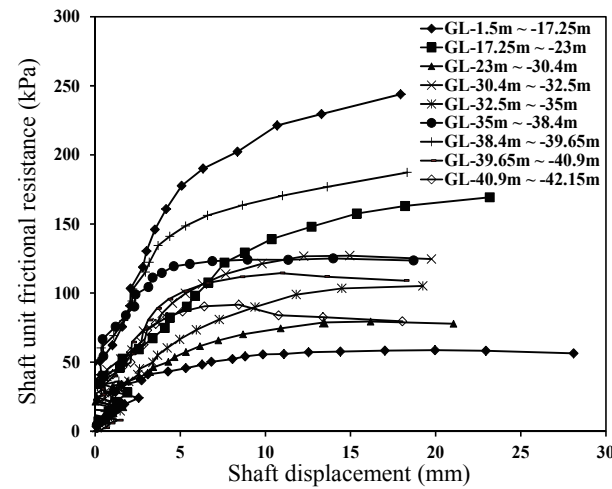


Fig. 5 Shaft unit frictional resistance versus displacement of pile C1

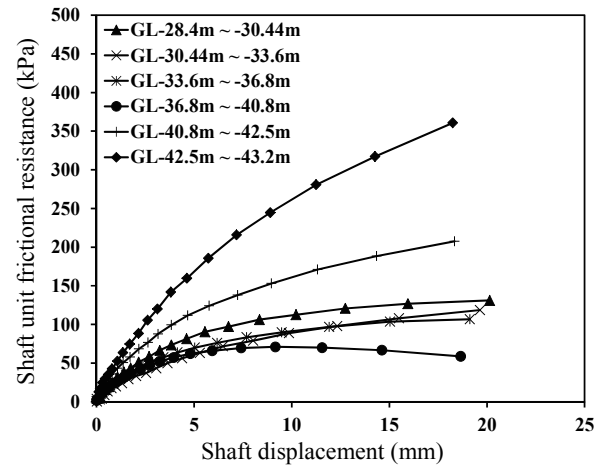


Fig. 6 Shaft unit frictional resistance versus displacement of pile C2

5. HYPERBOLIC MODEL

In order to simulate the axial side frictional resistance and the axial displacement relationships at different elevations of the test shafts, the hyperbolic model, used by Gupta (2012), is adopted in this paper. The hyperbolic function can be expressed as (Gupta 2012)

$$f_s = \frac{(\Delta/d)}{\frac{1}{G_i} + \frac{\Delta/d}{f_{su}}} \quad (1)$$

where f_s = side frictional resistance developed at any instant of time when the displacement of the barrette pile embedded in gravel at the depth of interest is Δ , d = equivalent diameter of the pile, f_{su} = ultimate side frictional resistance that could be reached before the asymptotic value and G_i = initial shear modulus.

Similar hyperbolic form has also been successfully used by Lin (1997) and Lin *et al.* (2014) to simulate the $t-z$ curves of the pile embedded in rock. Using transformed axes (Desai and Christian 1979), the hyperbolic model of Eq. (1) becomes linear when the ordinate equal to $1/G_i$ and the slope of the line as $1/f_{su}$. Variation of the parameter G_i at different depth reflects the initial stiffness of the behavior between the interface of the pile and the soil. In addition, the parameter f_{su} represents the ultimate side resistance of the considered depth.

The length of the test pile was subdivided into segments. G_i and f_{su} values determined from Δ/d versus f_s curves obtained from load tests are listed in Table 2. The simulated and the measured results for C1 and C2 at gravel layer is obtained as shown in Figs. 7(a) to 7(b), respectively. Since the measured data of C1 pile before 2 mm was so irregular, extrapolation of the measured curve beyond 2 mm to the origin of the curve was used to determine the G_i . The simulated curves provide information of both the initial shear modulus and the ultimate side frictional resistance, which could be used for further analysis of the pile.

Table 2 G_i and f_{su} values determined from Δ/d versus f_s curves

Shaft	Mid-depth (m)	G_i (kN/m^2)	f_{su} (kN/m^2)
C1	9.378	39969.25	61.15
	20.123	78950.04	206.98
	26.7	48445.08	93.62
	31.45	120353.50	142.27
	33.75	71355.49	118.05
	36.7	216326.90	127.86
	39.03	105366.80	225.18
	40.28	69009.53	132.90
	41.53	66021.74	97.43
	42.78	78823.09	328.27
C2	14.23	37517.32	79.19
	27.43	101317.10	1086.92
	29.42	88637.09	138.18
	32.02	35356.35	155.62
	35.2	52552.46	127.89
	38.8	76842.29	74.95
	41.65	66779.06	291.21
	42.85	91895.12	529.50

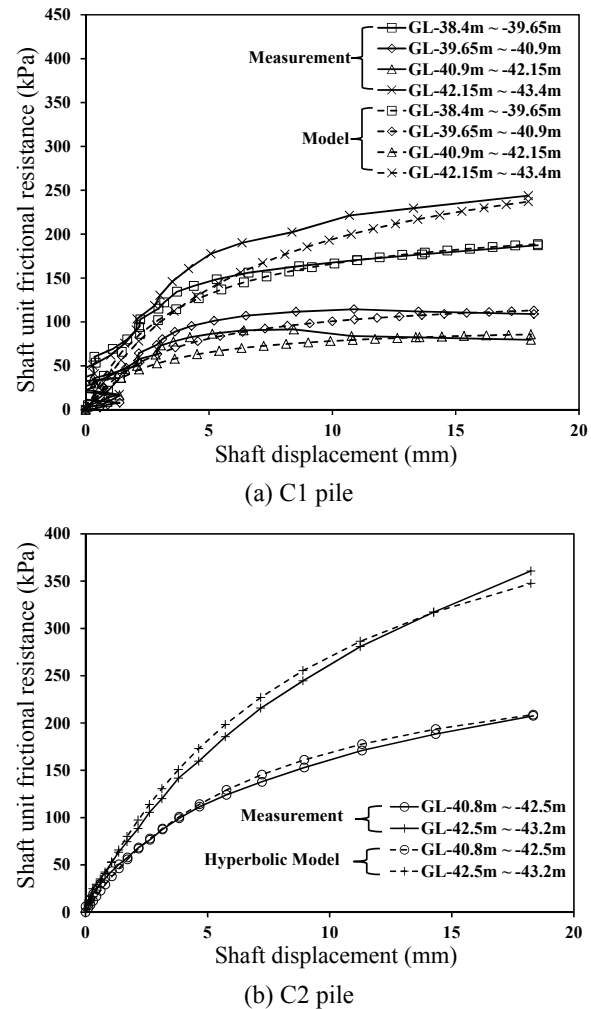


Fig. 7 The simulated and the measurement results of (a) C1 and (b) C2 piles at gravel layer

6. SUMMARY AND CONCLUSIONS

Axial pile load tests on performance of two barrette pile socket in gravel layer were carried out at two sites in Taipei. Based on the results of pile load test discussed in this paper, the following conclusions are drawn:

1. Although the C2 pile had shorter socket length into gravel layer, the load versus settlement relationship of the pile C2 was identical to that of the C1 pile, due to the toe grouting of C1 pile and possibly relatively higher SPT-N value of gravel layer at site 2.
2. Toe grouting improved not only the end bearing capacity but also the frictional resistance of both test piles.
3. Based on the De Beer and the Van der veen method, the ultimate capacity of the C1 pile is 35.28 MN and 41.16 MN, respectively. For C2 pile, the ultimate capacity is higher than 37.04 MN and 39.20 MN with respect to the De Beer and the Van der veen method.
4. The hyperbolic model provided a good fit with Δ/d versus f_s relationship obtained from load tests on instrumented piles. In addition, the model used for the pile load test data also provided reasonable estimate of G_i and f_{su} values in gravel layer.

ACKNOWLEDGEMENTS

The present study was carried out as part of a research project funded by the Ministry of Science and Technology of Taiwan (NSC 102-2221-E-019-028-MY3). The first author is grateful for the financial support.

REFERENCES

- American Society for Testing and Material (1994). *Standard Test Methods for Deep Foundations under Static Axial Compressive Load*, ASTM D1143, USA.
- De Beer, E.E. (1967). "Bearing capacity and settlement of shallow foundations on sand." *Proceeding of Bearing Capacity and Settlement of Foundations*, Duke University, Durham, N.C., 15–33.
- Desai, C.S. and Christian, J.T. (1977). *Numerical Methods in Geotechnical Engineering*, McGraw Hill, New York, USA.
- Gupta, R.C. (2012). "Hyperbolic model for load tests on instrumented drilled shafts in intermediate geomaterials and rock." *Journal of Geotechnical and Geoenvironmental Engineering*, ASCE, **138**(11), 1407–1414.
- Liao, J.C., Lin, S.S., Mulowayi, E., and Lin, Y.K., (2013). "Axial capacity of a rectangular pile socket in gravel layer." *Advances in Foundation Engineering*, Phoon, K.K., Chua, T.S., Yang, H., and Cham, W.M. Eds., Research Publishing, 467–471, Singapore.
- Lin, S.S. (1997). "Use of filamented beam elements for bored pile analysis." *Journal of Structural Engineering*, ASCE, **123**(9), 1236–1244.
- Lin, S.S., Yin, Y.L., Fu, K.C., Lin, Y.K., Kuo, C.J., and Chang, Y.H. (2014). "Effects of toe grouting on axial performance of rock socketed drilled shafts." *Geotechnical Engineering*, SEAGS/AGSSEA (accepted).
- O'Neill, M.W. and Reese, L.C. (1999). *Drilled Shafts: Construction Procedures and Design Methods*. Publication No. FHWA-IF-99-025, Department of Transportation, Washington D.C., USA.
- Rollins, K.M., Clayton, R.T., Mikesell, R.C., and Blaise, B.C. (2005). "Drilled shaft side friction in gravelly soils." *Journal of Geotechnical and Geoenvironmental Engineering*, ASCE, **131**(8), 987–1003.
- Stas, C.V. and Kulhawy, F.H. (1984). *Critical Evaluation of Design Methods for Foundations under Axial Uplift and Compression Loading*. Report El-3771, Electric Power Research Institute, Palo Alto, California, USA.
- Van der veen, C. (1953). "The bearing capacity of pile." *Proceedings of 3rd International Conference on Soil Mechanics and Foundation Engineering*, Switzerland, 84–90.

